

## ASYMMETRIC TRANSMISSION OF LINEARLY POLARIZED WAVES AND DYNAMICALLY WAVE ROTATION USING CHIRAL METAMATERIAL

**Furkan Dincer<sup>1</sup>, Cumali Sabah<sup>2,\*</sup>, Muharrem Karaaslan<sup>3</sup>, Emin Unal<sup>3</sup>, Mehmet Bakir<sup>3</sup>, and Utku Erdiven<sup>4</sup>**

<sup>1</sup>Department of Electrical and Electronics Engineering, Bitlis University, Bitlis 13000, Turkey

<sup>2</sup>Department of Electrical and Electronics Engineering, Middle East Technical University — Northern Cyprus Campus, Kalkanli, Guzelyurt, TRNC/Mersin 10, Turkey

<sup>3</sup>Department of Electrical and Electronics Engineering, Mustafa Kemal University, Iskenderun, Hatay 31200, Turkey

<sup>4</sup>Department of Physics, Cukurova University, Adana 01330, Turkey

**Abstract**—The asymmetric transmission of the linearly polarized waves at normal incidence through the lossy anisotropic chiral structure is demonstrated. The proposed chiral metamaterial structure is composed of bi-layered discontinuous cross-wire-strips, and it is utilized in order to realize polarization rotation. Firstly, the theoretical relations between the incident polarization and the polarization rotation are derived using transmission matrices. Secondly, a strong and dynamically asymmetric transmission of linearly polarized electromagnetic wave through the chiral metamaterial has been demonstrated for microwave region, both by simulation and experimentally. The experiment results are in good agreement with the simulation ones. It can be seen from the results that the proposed chiral metamaterial structure can be used to design novel polarization control devices for several frequency regions.

---

*Received 6 May 2013, Accepted 26 May 2013, Scheduled 31 May 2013*

\* Corresponding author: Cumali Sabah (sabah@metu.edu.tr).

## 1. INTRODUCTION

The concept of metamaterials (MTMs) has achieved a remarkable importance due to their unusual properties different from any conventional materials [1–9]. These materials are artificial structures that can be designed to show specific electromagnetic (EM) properties not commonly found in nature. The first metamaterial is fabricated in 2000 by Smith and Kroll [10] with periodically arranged inclusions composed of a split ring resonator and wire structures. MTMs provide many interesting applications, such as super lens [11], cloaking [12], and negative refraction [13], etc.

The motivation of this study is to investigate the asymmetric feature of chiral MTMs. Chirality yields a cross-coupling between the electric and magnetic fields, and therefore right- and left-hand circularly polarized waves possess different transmission coefficients. Chiral MTMs do not exhibit any mirror symmetry. They cannot be brought into congruence with its mirror image unless they are lifted off the substrate. So, these issues are potentially useful to manipulate the polarization states of EM waves [14–23].

Many studies focus on asymmetric transmission through MTMs in two opposite directions. Fedotov et al. [20] outlined that asymmetric phenomenon requires presence of simultaneous planar chirality and anisotropy in the structure and it involves no change in the direction of transmitted waves. This asymmetric transmission is irrelevant to the non-reciprocity of the Faraday effect in magneto-optical media [21]. Kang et al. [21] studied the relationship among the elements of transmission matrix, which allows asymmetrical transmission for linearly polarized EM wave. In 2011, Plum et al. [22] observed the asymmetric transmission in any lossy periodically structured plane for oblique incidence. In 2013, Cheng et al. [4] studied a double-layer split-ring resonator structure (chiral MTM) to obtain giant circular dichroism with asymmetric transmission. In addition, chiral symmetry provides asymmetric transmission and reflection of circularly polarized radiation penetrating the structure from opposite sides. The asymmetric transmission has an important role in many applications such as polarization conversion [2], transmission filter [2], etc.

In this paper, we theoretically and experimentally analyzed the asymmetric transmission and polarization rotation of bi-layered and discontinuous cross-wire-strips (CWSs). The proposed design exhibits directional selectivity, which appears during the transmission through chiral MTM slab at microwave frequencies. Also, the structure can dynamically control to the polarization rotation of the EM wave.

Besides, it can easily be retailored for the millimeter wave and optical frequency regions.

## 2. THEORETICAL ANALYSIS

Chiral MTMs with the exhibition of cross-coupling and cross-polarization conversion generally result in asymmetric transmission for forward and backward propagation of circularly polarized waves over certain frequency ranges. This asymmetric transmission provides a certain difference between the polarization states of the wave applied in opposite sides. For the theoretical analysis, we consider an incoming plane wave that propagates in  $+z$  direction with the time dependence of  $e^{-i\omega t}$  which is suppressed throughout this work [23–26];

$$\mathbf{E}_i(\mathbf{r}, t) = \begin{pmatrix} E_x \\ E_y \end{pmatrix} e^{ikz} \quad (1)$$

with angular frequency  $\omega$ , wave vector  $k$ , and complex amplitudes  $E_x$  and  $E_y$ . To understand polarization conversion, transmission ( $T$ ) matrix expression can be applied for the given electric field as follows [23–26];

$$\mathbf{E}_t(\mathbf{r}, t) = \begin{pmatrix} T_x \\ T_y \end{pmatrix} e^{ikz} \quad (2)$$

It is assumed that the medium is symmetrically embedded in dielectric medium (e.g., in vacuum). The  $T$ -matrix relates the complex amplitudes of the incident field to that of the transmitted field:

$$\begin{pmatrix} T_x \\ T_y \end{pmatrix} = \begin{pmatrix} T_{xx} & T_{xy} \\ T_{yx} & T_{yy} \end{pmatrix} \begin{pmatrix} E_x \\ E_y \end{pmatrix} = \hat{T}_{lin}^f \begin{pmatrix} E_x \\ E_y \end{pmatrix} \quad (3)$$

The indices  $f$  and  $lin$  indicate propagation in forward direction and a special linear base with base vectors parallel to the coordinate axes, i.e., decomposing the incident wave-into  $x$  and  $y$  polarized components. The transmitted wave in  $x$  and  $y$  directions are  $T_{xx}$  and  $T_{yx}$ , respectively. Circularly polarized transmitted waves can be retrieved from the linear transmission coefficients  $T_{xx}$  and  $T_{yx}$  as [21–28];

$$T_{\pm} = T_{xx} \pm iT_{yx} \quad (4)$$

Four circular transmission coefficients  $T_{++}$ ,  $T_{-+}$ ,  $T_{+-}$ , and  $T_{--}$  can be calculated from the transmission and reflection coefficients of linearly polarized waves using the following equation in  $\pm z$  direction [21–28];

$$T_{circ}^f = \begin{pmatrix} T_{++} & T_{+-} \\ T_{-+} & T_{--} \end{pmatrix} \quad \& \quad T_{circ}^b = \begin{pmatrix} T_{++} & T_{-+} \\ T_{+-} & T_{--} \end{pmatrix} \quad (5)$$

If the propagation is along  $-z$  direction, the equations become [21, 24];

$$\begin{pmatrix} T_{++} & T_{+-} \\ T_{-+} & T_{--} \end{pmatrix} = \frac{1}{2} \begin{pmatrix} T_{xx} + T_{yy} + i(T_{xy} - T_{yx}) & T_{xx} - T_{yy} + i(T_{xy} + T_{yx}) \\ T_{xx} - T_{yy} - i(T_{xy} + T_{yx}) & T_{xx} + T_{yy} - i(T_{xy} - T_{yx}) \end{pmatrix} \quad (6)$$

The asymmetric transmission of the linearly and circularly polarized waves is commonly characterized by a parameter of  $\Delta$ . This parameter is defined as the difference between the transmittances in  $+z$  and  $-z$  directions. It can be used to represent the degree of asymmetric transmission. For linearly and circularly polarized waves, the asymmetric transmission parameter  $\Delta$  is defined as  $\Delta_{lin}^{(x)} = |T_{yx}|^2 - |T_{xy}|^2 = -\Delta_{lin}^{(y)}$ ,  $\Delta_{circ}^{(+)} = |T_{-+}|^2 - |T_{+-}|^2 = -\Delta_{circ}^{(y)}$  [21–26]. From Eqs. (3)–(6), it can be found that the asymmetric transmission for linear polarization can only be realized when the following condition is satisfied as  $|T_{yx}| \neq |T_{xy}| \cap T_{xx} = T_{yy}$  [21]. Planar MTMs always provide mirror symmetry in the propagation direction. Therefore, the components of the transmission matrix always support  $T_{xy} = T_{yx}$ . However, hybridized MTMs cause to break the mirror symmetry of the MTM structure in the propagation direction [21–23].

In addition, the polarization conversion features of the chiral MTM structures cause to change of polarization state of waves when propagating through the structure. This can be defined as optical activity for chiral structures. When a linearly polarized EM wave propagates in a medium, the azimuth of polarization plane rotates clockwise or counter-clockwise depending on the handedness of the material. This phenomenon provides the optical activity. These are the additional beneficial features of the chiral MTM structures.

### 3. DESIGN, SIMULATION, AND EXPERIMENT

The designed structure consists of bi-layered and discontinuous CWS structures (metallic part). The mentioned metallic part is placed on the front- and back-side of a host dielectric substrate and the overall structure (substrate with the metallic part) will provide asymmetric transmission for linearly polarized EM waves. Besides, the proposed structure can also provide asymmetry by changing the dimensions of CWSs such as length of and distances between the strips.

FR4 dielectric substrate is chosen as a host material with a thickness of  $a_4 = 1.6$  mm, relative permittivity of 4.2, and loss tangent of 0.02. CWSs are made of copper with a thickness of 0.036 mm and the conductivity of  $5.8 \times 10^7$  S/m. Figure 1 shows the structure in

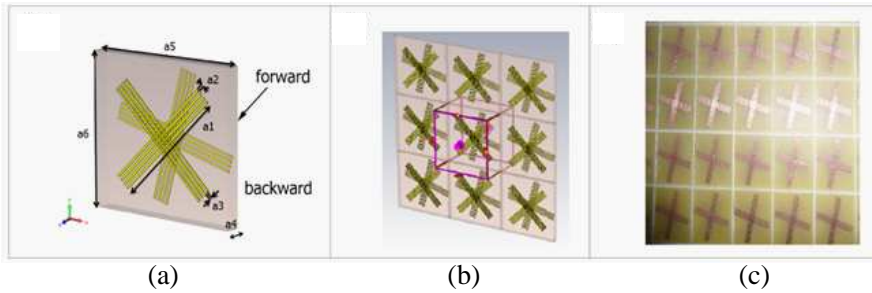


**Figure 1.** Bi-layered and discontinuous CWSs. (a) Dimensions of the unit-cell. (b) Unit cell with open add space boundary conditions. (c) Picture of the sample.

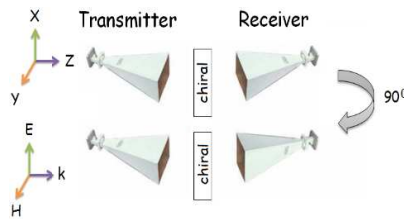


**Figure 2.** Schematics of the measurement method in the experiment [29].

detail. Figure 1(a) shows the schematic diagram of the unit cell. The line-width and height of the metallic strips are  $a_2 = 0.25$  mm and  $a_1 = 14$  mm, respectively. The gap in CWSs is  $a_3 = 0.25$  mm. The offsets with respect to the origin are  $45^\circ$  for the front CWSs and  $75^\circ$  for the back CWSs, respectively.

The structure was simulated and analyzed with a commercial full-wave EM solver (CST Microwave Studio based on finite integration technique). Unit cell and open add space boundary conditions are used in the simulation as shown in Figure 1(b). The fabricated sample with the dimension of  $240 \times 240$  mm<sup>2</sup> is shown in Figure 1(c). The unit cell has periodicity of  $a_5 = a_6 = 16$  mm along  $x$ - and  $y$ -directions. CWSs have strong feature to rotate polarization of EM wave due to the electric and magnetic coupling between multi cross-strips.

The numerical simulations are analyzed then to determine reflection and transmission properties of the proposed structure. Figure 2 shows the schematic experimental setup for the measurement of  $T_{xx}$  and  $T_{yx}$ . The experimental measurement setup consists of an Agilent-E5071B ENA RF vector network analyzer (VNA) and

microwave horn antennas. Firstly, free space measurement without the chiral structure is carried out and this measurement used as the calibration data for VNA. Secondly, the structure is then inserted into the experimental measurement setup and transmission measurements are performed. The distance between the horn antennas and chiral slab is kept sufficiently large to eliminate near-field effects.

#### 4. NUMERICAL AND EXPERIMENTAL RESULTS

In order to investigate the frequency response of the chiral MTM, the structure is designed and simulated with respect to the plane waves propagating along  $(+z)$  and  $(-z)$  directions. Then, to obtain linear  $T$ -matrix coefficients of the slab,  $T_{xx}$  and  $T_{yx}$  are obtained from the simulations and experiments when the incident wave is  $x$ -polarized. After that, linear transmission  $T_{xy}$  and  $T_{yy}$  are obtained for  $y$ -polarized incident wave, too.

We measured both the forward and backward transmission coefficients. Figure 3 shows the measurement and simulation results of  $T$ -matrix elements ( $T_{xx}$ ,  $T_{xy}$ ,  $T_{yx}$ ,  $T_{yy}$ ) of the slab for propagations of forward  $(+z)$  and backward  $(-z)$  directions. The experimental results are in good agreement with the numerical simulations as shown. It can be seen that the co-polarized transmission  $T_{yy}$  has a resonant peak and reaches its maximum value of around 0.66 at the frequency of  $f = 6.91$  GHz. Also, the simulation and experimental results show that  $T_{xx}$  and  $T_{yy}$  are almost equal to each other. Cross-polarized

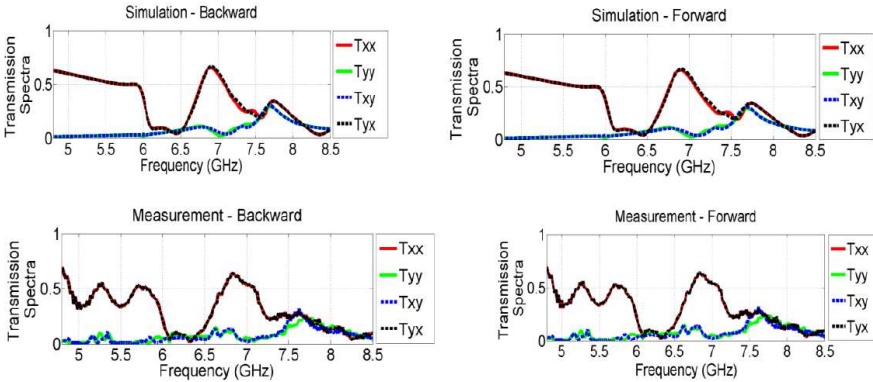


**Figure 3.** Simulated and measured transmission spectra of  $T$ -matrix elements ( $T_{xx}$ ,  $T_{xy}$ ,  $T_{yx}$ ,  $T_{yy}$ ) of the slab for propagations of  $+z$  (forward) and  $-z$  (backward) directions.

transmission  $T_{xy}$  and  $T_{yx}$  reduce to its minimum value of about 0.01 at the frequency of  $f = 4.8$  GHz.

According to the simulated and experimental results (and Eq. (8) too), asymmetry in the transmission for the linear polarization may be acquired when the propagation direction is reversed. This change confirms the presence of circular conversion of dichroism  $T_{+-} \neq T_{-+}$ . However, the conventional optical activity is independent from the propagation direction ( $T_{+-} = T_{-+}$ ). Also, replacing the planar chiral metamaterial with its mirror image reverses the asymmetry of circular transmission. Therefore, when handedness of the polarization state is changed, the sign of the transmission asymmetry will be reversed for asymmetric planar chiral MTMs. Moreover, it can be seen that when the propagation direction is reversed, the cross-polarization elements  $T_{xy}$  and  $T_{yx}$  interchange with each other (Figure 3). Normally, any planar MTM always has mirror symmetry in the propagation direction. As studied in the theoretical analysis,  $T_{xx}$  and  $T_{yy}$  are exactly equal, which ensures zero asymmetric transmission of circular polarization waves for chiral MTMs that is satisfied both in the simulation and experimental results (Figure 3) [16–26].

The asymmetric transmission parameter  $\Delta$  is calculated and normalized using Eqs. (8)–(9) for both linear and circular polarizations as shown in Figure 4. It can be seen that the proposed structure exhibits asymmetric transmission at two different frequencies, namely at 6.94 GHz and 7.64 GHz for linear polarization. No change is observed in  $\Delta$  ( $\approx 0$ ) for the circular polarization which is commonly known for this kind of chiral MTM structures. In simulation, the value of  $\Delta$  parameter for linear polarizations reaches to 0.25 at 6.94 GHz. Especially, asymmetric transmission is approximately 0.875 at 7.64 GHz. The corresponding experimental values are low when compared with the simulation results. The discrepancies can be imputed to fabrication tolerances related to the etching process and the dielectric dispersion of the substrate used. As seen, the proposed chiral MTM structure has relatively large asymmetric transmission

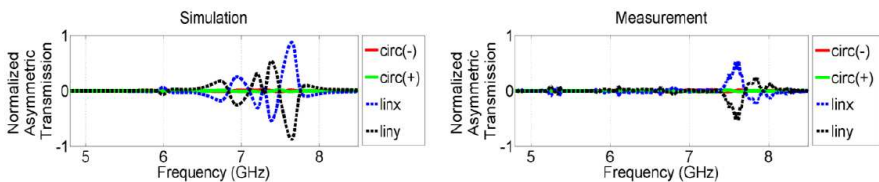


**Figure 4.** Simulation and measurement results of asymmetric transmission ( $\Delta$ ) parameter for linear and circular polarizations.

parameter for linear polarization. This feature can also be observed for different frequencies.

After obtaining transmission data, the retrieval study for the chirality parameter,  $\kappa$ , is applied. Complex chirality can be obtained directly from transmission coefficients as  $\text{Re}(\kappa) = \frac{[\arg(T+) - \arg(T-) + 2m\pi]}{2k_0d}$ ,  $\text{Im}(\kappa) = \frac{\ln|T_L| - \ln|T_R|}{2k_0d}$ , where  $k_0$  is the wave number in vacuum,  $d$  the thickness of the structure, and  $m$  is integer [27–31]. Figure 5 shows the simulation and measurement results for the chirality parameter. The chirality is large,  $\kappa = \pm 6.1$  (4.7) at the frequency of 8.36 GHz for the simulation (measurement) results. Furthermore, the chirality is larger,  $\kappa = \pm 7.7$  at the frequency of  $f = 6.46$  GHz for the simulation. The corresponding positive chirality value for the frequency span of 6.1 GHz and 6.5 GHz is approximately 6 for the measurement. However, the negative value is small when compared with the simulation and reaches to  $-2$ , for the measurement.

In order to check the performance of the designed structure based on chirality, the Figure of Merit ( $FOM = |\text{Re}(\kappa)/\text{Im}(\kappa)|$ ) calculation is performed and the result is shown in Figure 6. As seen, FOM values at and around the resonances of 6.46 GHz and 8.36 GHz (when the chirality changes significantly) are very large. This implies very good performance of the proposed structure.

Now, the effect of the change in the dimensions of CWSs on the chirality is investigated and the results are shown in Figure 7.

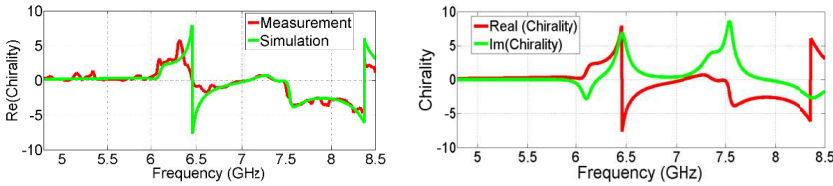


**Figure 5.** Simulated and measured chirality parameter for fabricated chiral MTM structure.

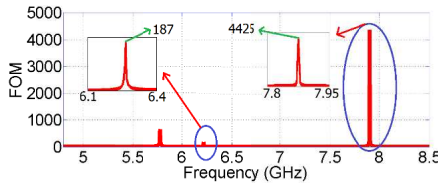


**Figure 6.** Figure of merit of the proposed chiral MTM.



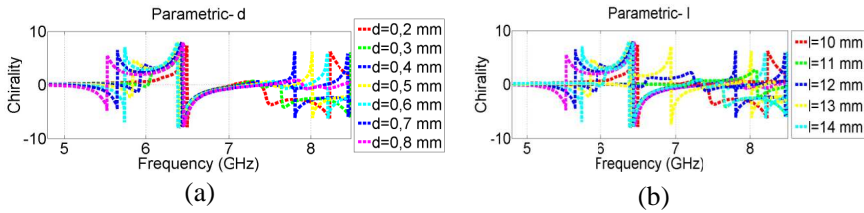


**Figure 7.** Simulations results for the chirality parameter for different dimensions of CWSs. (a) Results for the changes of the gap distance between CWSs. (b) Results for the variation of the length of CWSs.

When the gap (distance between CWSs) is increased from 0.20 mm to 0.80 mm and the length of CWSs are increased from 10 mm to 14 mm, reconfigurable chirality can be obtained. As seen, there are up- and down-shifts in the frequency response of the chirality when the dimensions of CWSs varied. This provides non-dynamic (mechanical) tunability and flexibility to obtain desired chirality by varying the dimensions of CWSs.

In order to verify the character of the resonance(s) for the proposed design, the surface current distributions are presented which are shown in Figure 8. Notice, at the frequency of 8.36 GHz, the antiparallel current distribution exists on the top and bottom layer of CWSs, which is asymmetric resonance mode and directly related with the magnetic resonance (see Refs. [27, 28] for details). This means the resonance at 8.36 GHz is induced by the magnetic field. On the other hand, the structure provides a parallel current distribution flowing on two layers of CWSs at 6.46 GHz, which is the symmetric resonance mode and excited by the electric field [27, 28]. The proposed geometry provides parallel and antiparallel current distributions (symmetric and asymmetric resonance modes) at two different frequencies which is an indication to recognize the structure as a chiral MTM [16, 27–30].

As a further investigation, the magnetic and electric field distributions at the resonances (for 8.36 GHz and 6.46 GHz, respectively) is analyzed which are shown in Figure 9. The current distribution and the magnetic field for 8.36 GHz is compatible with each other as seen Figure 8 and Figure 9. High concentration of the magnetic field around CWSs confirms asymmetric resonance mode which is excited by the magnetic dipoles. Moreover, the physical mechanism of the resonance mode for 6.46 GHz is different than that of 8.36 GHz. The electric field distribution of the structure at 6.46 GHz validates the symmetric current which is created by the coupling of the electric dipoles [16, 27–30].

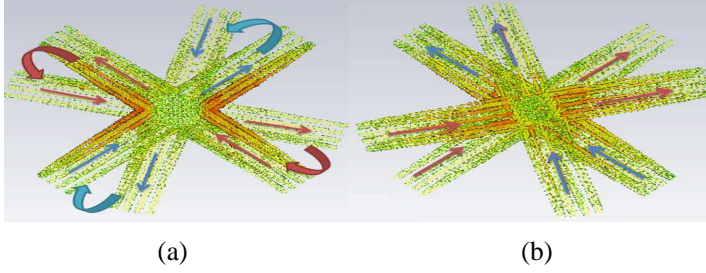


**Figure 8.** The simulated surface current distribution (a) at the magnetic resonance of 8.36 GHz and (b) at the electric resonance frequency of 6.46 GHz.

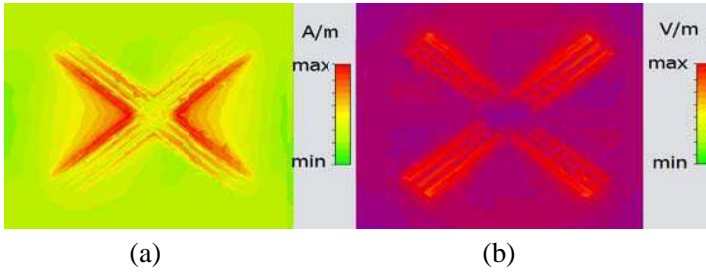


**Figure 9.** (a) Magnetic field distribution of the structure at the resonant frequency of 8.36 GHz and (b) electric field distribution of the structure at the resonant frequency of 6.46 GHz.

## 5. CONCLUSIONS

Theoretical and experimental analysis of a chiral MTM structure composed of a dielectric substrate and bi-layered and discontinuous CWSs for asymmetric transmission is investigated in detail. The proposed structure can generate an asymmetric EM wave transmission for linear polarization. In addition, the structure has flexible, tunability, and easy fabrication features. The angle, length, width, and distance of the wire strips can be retailored for desired EM response such as asymmetric transmission (as mentioned), different chirality parameters, and so on. These controllable features can also provide significant optical activity because of the internal property of chiral metamaterial. Besides, the structure's polarization tunability offers an additional degree of freedom for the polarization control in which the strong optical activity can be utilized to design new microwave

rotator or polarization control devices. This is confirmed with the good agreement between the simulated and experimental results. Note that the design of novel devices based on the findings of the present study as well as the study itself can easily be extended for different frequency regimes too.

Therefore, bi-layered and discontinuous CWSs-shaped topology lends itself as a useful alternative to the well-known chiral MTM structures which provides asymmetric transmission and opens a way to design new devices with very large-chirality to be used in several potential applications. Particularly, the structure can be utilized to design more efficient circulators, configurable polarization rotator, wave-plates and sensors.

## REFERENCES

1. Sabah, C., H. T. Tastan, F. Dincer, K. Delihacioglu, M. Karaaslan, and E. Unal, "Transmission tunneling through the multi-layer double-negative and double-positive slabs," *Progress In Electromagnetics Research*, Vol. 138, 293–306, 2013.
2. Sabah, C. and H. G. Roskos "Design of a terahertz polarization rotator based on a periodic sequence of chiral metamaterial and dielectric slabs," *Progress In Electromagnetics Research*, Vol. 124, 301–314, 2012.
3. Dong, J. F., "Surface wave modes in chiral negative refraction grounded slab waveguides," *Progress In Electromagnetics Research*, Vol. 95, 153–166, 2009.
4. Cheng, Y., Y. Nie, L. Wu, and R. Gong, "Giant circular dichroism and negative refractive index of chiral metamaterial based on splitting resonators," *Progress In Electromagnetics Research*, Vol. 138, 421–432, 2013.
5. Burlak, G., "Spectrum of Cherenkov radiation in dispersive metamaterials with negative refraction index," *Progress In Electromagnetics Research*, Vol. 132, 149–158, 2012.
6. Da, H. and C. W. Qiu, "Graphene-based photonic crystal to steer giant Faraday rotation," *Appl. Phys. Lett.*, Vol. 100, 241106, 2012.
7. Faruque, M. R. I., M. T. Islam, and N. Misran, "Design analysis of new metamaterial for EM absorption reduction," *Progress In Electromagnetics Research*, Vol. 124, 119–135, 2012.
8. Chen, H. S., L. Huang, X. X. Cheng, and H. Wang, "Magnetic properties of metamaterial composed of closed rings," *Progress In Electromagnetics Research*, Vol. 115, 317–326, 2011.

9. Karaaslan, M. and F. Karadag, "Adjustable sub-wavelength waveguide by uniaxially designed artificial magnetic media," *Optoelectron. Adv. Mat.*, Vol. 3, 578–580, 2009.
10. Smith, D. R. and N. Kroll, "Negative refraction index in left-handed materials," *Phys. Rev. Lett.*, Vol. 85, 2933–2936, 2000.
11. Fang, N., H. Lee, C. Sun, and X. Zhang, "Sub-diffraction-limited optical imaging with a silver superlens," *Science*, Vol. 308, 534–537, 2005.
12. Pendry, J. B., D. Schurig, and D. R. Smith, "Controlling electromagnetic fields," *Science*, Vol. 312, 1780–1782, 2006.
13. Shelby, R. A., D. R. Smith, and S. Schultz, "Experimental verification of a negative index of refraction," *Science*, Vol. 292, 77–79, 2001.
14. He, Y., J. Shen, and S. He, "Consistent formalism for the momentum of electromagnetic waves in lossless dispersive metamaterials and the conservation of momentum," *Progress In Electromagnetics Research*, Vol. 116, 81–106, 2011.
15. Zhang, F., V. Sadaune, L. Kang, Q. Zhao, J. Zhou, and D. Lippens, "Coupling effect for dielectric metamaterial dimer," *Progress In Electromagnetics Research*, Vol. 132, 587–601, 2012.
16. Zhao, R., L. Zhang, J. Zhou, T. Koschny, and C. M. Soukoulis, "Conjugated gammadion chiral metamaterial with uniaxial optical activity and negative refractive index," *Phys. Rev. B*, Vol. 83, 035105-4, 2011.
17. Sabah, C. and S. Uckun, "Multilayer system of Lorentz/Drude type metamaterials with dielectric slabs and its application to electromagnetic filters," *Progress In Electromagnetics Research*, Vol. 91, 349–364, 2009.
18. Iwanaga, M., "First-principle analysis for electromagnetic eigen modes in an optical metamaterial slab," *Progress In Electromagnetics Research*, Vol. 132, 129–148, 2012.
19. Yan, S. and G. A. E. Vandenbosch, "Increasing the NRI bandwidth of dielectric sphere-based metamaterials by coating," *Progress In Electromagnetics Research*, Vol. 132, 1–23, 2012.
20. Fedotov, V. A., P. L. Mladyonov, S. L. Prosvirnin, A. V. Rogacheva, Y. Chen, and N. I. Zheludev, "Asymmetric propagation of electromagnetic waves through a planar chiral structure," *Phys. Rev. Lett.*, Vol. 97, 167401-4, 2006.
21. Kang, M., J. Chen, H.-X. Cui, Y. Li, and H.-T. Wang, "Asymmetric transmission for linearly polarized electromagnetic radiation," *Opt. Express*, Vol. 19, 8347–8356, 2011.

22. Plum, E., V. A. Fedotov, and N. I. Zheludev, "Asymmetric transmission: A generic property of two-dimensional periodic patterns," *J. Optics*, Vol. 13, 024006-6, 2011.
23. Guo, W., L. He, B. Li, T. Teng, and X. W. Sun, "A wideband and dual-resonant terahertz metamaterial using a modified SRR structure," *Progress In Electromagnetics Research*, Vol. 134, 289–299, 2013.
24. Menzel, C., C. Helgert, C. Rockstuhl, and E. B. Kley, A. Tünnermann, T. Pertsch, and F. Lederer, "Asymmetric transmission of linearly polarized light at optical metamaterials," *Phys. Rev. Lett.*, Vol. 104, 253902-4, 2010.
25. Huang, C., Y. Feng, J. Zhao, Z. Wang, and T. Jiang, "Asymmetric electromagnetic wave transmission of linear polarization via polarization conversion through chiral metamaterial structures," *Phys. Rev. B*, Vol. 85, 195131-5, 2012.
26. Huang, C., J. Zhao, T. Jiang, and Y. Feng, "Asymmetric transmission of linearly polarized electromagnetic wave through chiral metamaterial structure," *Journal of Electromagnetic Waves and Applications*, Vol. 26, Nos. 8–9, 1192–1202, 2012.
27. Wang, B., J. Zhou, T. Koschny, M. Kafesaki, and C. M. Soukoulis, "Chiral metamaterials: Simulations and experiments," *Journal of Optics A: Pure and Applied Optics*, Vol. 11, 114003-13, 2009.
28. Zhou, J., J. Dong, B. Wang, T. Koschny, M. Kafesaki, and C. M. Soukoulis, "Negative refractive index due to chirality," *Phys. Rev. B*, Vol. 79, 121104-4, 2009.
29. Li, Z., M. Mutlu, and E. Ozbay, "Chiral metamaterials: From optical activity and negative refractive index to asymmetric transmission," *J. Optics*, Vol. 15, 023001, 2013.
30. Li, Z., H. Caglayan, E. Colak, J. Zhou, C. M. Soukoulis, and E. Ozbay, "Coupling effect between two adjacent chiral structure layers," *Opt. Express*, Vol. 18, 5375–5383, 2010.
31. Li, Z., R. Zhao, T. Koschny, M. Kafesaki, K. B. Alici, E. Colak, H. Caglayan, E. Ozbay, and C. M. Soukoulis, "Chiral metamaterials with negative refractive index based on four 'U' split ring resonators," *Appl. Phys. Lett.*, Vol. 97, 081901-3, 2010.